The Journal of Chemical Physics

RESEARCH ARTICLE | JUNE 02 2014

Mixtures of protic ionic liquids and molecular cosolvents: A molecular dynamics simulation

Borja Docampo-Álvarez; Víctor Gómez-González; Trinidad Méndez-Morales; Jesús Carrete; Julio R. Rodríguez; Óscar Cabeza; Luis J. Gallego; Luis M. Varela

Check for updates

J. Chem. Phys. 140, 214502 (2014)
https://doi.org/10.1063/1.4879660

View Online
Export Citation

Articles You May Be Interested In

Structure and dynamics of propylammonium nitrate-acetonitrile mixtures: An intricate multi-scale system probed with experimental and theoretical techniques

J. Chem. Phys. (April 2018)

Molecular heterogeneity in aqueous cosolvent systems

J. Chem. Phys. (May 2020)

Nanostructured solvation in mixtures of protic ionic liquids and long-chained alcohols

J. Chem. Phys. (March 2017)

24 February 2026 13:02:40

Zurich Instruments

Freedom to Innovate.

The New VHFLI 200 MHz Lock-in Amplifier.

Orchestrate pulses, triggers, and acquisition as the hub of your experiment.
Discover more – run every signal analysis tool, simultaneously.

Order now

AIP Publishing

Mixtures of protic ionic liquids and molecular cosolvents: A molecular dynamics simulation

Borja Docampo-Álvarez,[1,a)] Víctor Gómez-González,[1] Trinidad Méndez-Morales,[1] Jesús Carrete,[1,2] Julio R. Rodríguez,[1] Óscar Cabeza,[3] Luis J. Gallego,[1] and Luis M. Varela[1,b)]

[1]*Grupo de Nanomateriais e Materia Branda, Departamento de Física da Materia Condensada, Universidade de Santiago de Compostela, Campus Vida s/n E-15782, Santiago de Compostela, Spain*
[2]*LITEN, CEA-Grenoble, 17 rue des Martyrs, BP166, F-38054, Grenoble, Cedex 9, France*
[3]*Facultade de Ciencias, Universidade da Coruña, Campus A Zapateira s/n E-15008, A Coruña, Spain*

(Received 26 February 2014; accepted 13 May 2014; published online 2 June 2014)

In this work, the effect of molecular cosolvents (water, ethanol, and methanol) on the structure of mixtures of these compounds with a protic ionic liquid (ethylammonium nitrate) is analyzed by means of classical molecular dynamics simulations. Included are as-yet-unreported measurements of the densities of these mixtures, used to test our parameterized potential. The evolution of the structure of the mixtures throughout the concentration range is reported by means of the calculation of coordination numbers and the fraction of hydrogen bonds in the system, together with radial and spatial distribution functions for the various molecular species and molecular ions in the mixture. The overall picture indicates a homogeneous mixing process of added cosolvent molecules, which progressively accommodate themselves in the network of hydrogen bonds of the protic ionic liquid, contrarily to what has been reported for their aprotic counterparts. Moreover, no water clustering similar to that in aprotic mixtures is detected in protic aqueous mixtures, but a somehow abrupt replacing of $[NO_3]^-$ anions in the first hydration shell of the polar heads of the ionic liquid cations is registered around 60% water molar concentration. The spatial distribution functions of water and alcohols differ in the coordination type, since water coordinates with $[NO_3]^-$ in a bidentate fashion in the equatorial plane of the anion, while alcohols do it in a monodentate fashion, competing for the oxygen atoms of the anion. Finally, the collision times of the different cosolvent molecules are also reported by calculating their velocity autocorrelation functions, and a caging effect is observed for water molecules but not in alcohol mixtures. © *2014 AIP Publishing LLC*. [http://dx.doi.org/10.1063/1.4879660]

24 February 2026 13:02:40

I. INTRODUCTION

The interest in ionic liquids (ILs), systems that are composed entirely of ions and are fluids at room temperature, has rapidly grown in the recent years, not only due to their wide range of existing and potential applications (catalysis, electrochemical devices, extraction, and separation processes and, among others, nuclear industry),[1–4] but also due to their unusual and tunable physical properties (negligible vapor pressure, high ionic conductivity, large temperature stability range, large liquidus range, and very good solvent properties).[5–8]

A subset of ILs that stand out because of their characteristic features are protic ionic liquids (PILs), prepared through a simple neutralization reaction between a Brønsted acid and a Brønsted base.[9–12] This transfer of a proton distinguishes PILs from aprotic ionic liquids (AILs) and gives them the capability of hydrogen bonding; it also makes them suitable for various electrochemical applications such as electrolytes for fuel cells, double-layer capacitors and, since very recently, lithium-ion batteries.[11,13–17]

The most widely investigated PIL is ethylammonium nitrate (EAN), which is also the first known IL and dates from 1914, when Walden described it as an IL with a melting point of 287.6 K.[18] However, despite their having been discovered a century ago and their numerous potential applications, the number of studies regarding the properties of PILs is not yet comparable to those analyzing the behavior of AILs. In particular, several experimental studies can be found in the bibliography,[19–30] many of which have been reported by Greaves *et al.*[9,12,31,32] and, to a much smaller scale, some computational works have been performed to better understand this kind of systems.[33–38]

ILs are usually placed in a new class of "designer solvents" due to their unique properties and the virtually infinite amount of combinations that could be formed with cations and anions. However, their usage in synthesis and extraction processes requires knowledge about their miscibility with other solvents and about the behavior of the products of reactions in these systems (indeed, several reviews have been published that tackle these mixtures; see e.g., Ref. 39). In this respect, a key factor in PILs is proton transfer that leads to the presence of proton-donor and proton-acceptor sites. A typical consequence is the presence of a strong three-dimensional hydrogen bond network in their bulk similar to the tetrahedral one that can be found in bulk water.[40] Because of this reason,

a)Borja Docampo-Álvarez and Víctor Gómez-González contributed equally to this work.
b)Author to whom correspondence should be addressed. Electronic mail: luismiguel.varela@usc.es

 © 2014 AIP Publishing LLC

it is interesting to analyze the behavior of mixtures of PILs and molecular solvents with variable ability to form hydrogen bonds, including water[41,42] and short-chained alcohols,[43–46] and shed some light on the evolution of the hydrogen bond networks in this kind of solutions. However, up to date only a limited number of articles have reported the structural and thermodynamic properties of these mixtures.[47–53] As an example, Greaves *et al.* investigated the effect of adding water and primary *n*-alcohols on the nanoscale structure of several PILs by means of small- and wide-angle X-ray scattering (SWAXS).[54,55] In the first case, they found that the aggregate structure of the neat PILs is retained up to high concentrations of water, showing that water molecules can be localized in the ionic region and its addition to the PILs has little effect on the nonpolar domains. However, in Ref. 55 Greaves *et al.* reported that those molecular solvents with both hydrophobic and hydrophylic moieties (such as primary alcohols) can have a significant impact on the nonpolar regions of the PILs, and that this effect depends on the relative alkyl chain lengths of the alcohol and the PIL. In addition, Hayes *et al.*[56] also analyzed the bulk solvent structure of mixtures of EAN and water by using SWAXS. Their work led to the conclusion that water changes the EAN nanostructure mainly due to its interaction with the charged group of the ions and the corresponding increase of the effective head group size of the cation.

However, it must be said that, surprisingly enough, we are not aware of any computational reports on the nanostructure of mixtures of PILs with water or other organic solvents up to now. Understanding the behavior of ILs at the microscopic level is crucial in order to predict their physicochemical properties and their suitability for a given application. Thus, given the normally difficult access to these properties from an experimental point of view, molecular dynamics (MD) simulations can be considered as a fundamental tool for the study of these systems at a molecular level.

In this paper, the effect of adding water and the short-chained alcohols methanol and ethanol on the structure of EAN at room temperature has been investigated over the whole miscibility ranges of the corresponding mixtures. The change of several properties such as density, radial distribution functions (rdfs), coordination numbers, spatial distribution functions, hydrogen bonds, and velocity autocorrelation functions with the addition of the three aforementioned solvents was observed and compared to obtain further information of the nanostructure of these systems.

The remainder of this paper is organized as follows. The methodology and computational details, together with some preliminary experimental measurements, are given in Sec. II. In Sec. III, we present and discuss our results, and in Sec. IV we summarize our main conclusions.

II. EXPERIMENTAL AND COMPUTATIONAL SECTION

A. Chemicals and density measurements

EAN was purchased from IOLITEC with purity degrees of >97% and it was used as received. Methanol and ethanol (absolute) were provided by Prolabo with a purity >99.9% and >99.8%, respectively, and the employed water was de-ionized and distilled. Density was continuously and automatically measured at 298.15 K using a DSA 5000 Anton Paar density and sound velocity analyzer. This device is equipped with a latest-generation vibrating tube for density measurements with a resolution of $\pm 10^{-6}$ g cm^{-3}. Temperature was controlled to within $\pm 10^{-3}$ K by means of a Peltier module. The density meter was calibrated with dry air and distilled water at known pressure and temperature.

B. Simulation details

We carried out MD simulations of neat EAN and its mixtures with water and alcohols (ethanol and methanol) at $T = 298.15$ K and $P = 1$ atm by using the GROMACS 4.5.4 package and a standard MD all-atom force field, OPLS-AA.[57] We modelled each nitrate anion as a set of seven sites, three of them "heavy" sites carrying mass but not taking direct part in interactions, and the remaining four virtual interaction sites with no mass. The masses and positions of heavy sites were chosen so as to preserve the total mass, center of mass, and moment of inertia of a $[NO_3]^-$ anion. Virtual interaction sites were assigned partial charges of $q_N = +0.794$ for the nitrogen atom and $q_O = -0.598$ for the oxygen atoms,[58] whose Lennard-Jones (LJ) parameters are, respectively, $\sigma_N = 3.496 \times 10^{-1}$ nm, $\varepsilon_N = 7.1128 \times 10^{-1}$ kJ/mol, $\sigma_O = 3.175 \times 10^{-1}$ nm, and $\varepsilon_O = 8.7864 \times 10^{-1}$ kJ/mol. These parameters were fitted to reproduce the experimental density of pure EAN. Regarding the parameters for water, we employed the TIP5P model of Mahoney and Jorgensen,[59] which, in addition to the LJ center placed on the oxygen and the charges located at the hydrogen atoms, places two partial charges representing the lone pairs of the oxygen atom. Finally, both alcohols were represented by means of the molecular model proposed by Jorgensen.[60] The remaining details of the simulation have been reported in Ref. 61. Since solubility is guaranteed over the whole composition range, the solvent molar percentages simulated were $\%_{solvent} = \{0, 5, 15, 25, 50, 75, 80, 85, 90, 95, \text{and } 98\}$. The initial configurations for most of the molar percentages were obtained by randomly inserting 300 ionic pairs of EAN in a cubic box in order to get trajectories yielding statistically meaningful results, whereas for $\%_{solvent} = \{5, 95, \text{and } 98\}$ we considered 950, 50, and 50 ionic pairs, respectively. The number of solvent molecules was adjusted in each case by considering each ionic pair as a single unit in the calculations. To avoid overlap between molecules, an insertion was rejected if one of the new atoms is placed closer than 0.25 nm of any of the atoms that already exist in the box. The initial volume of the cubic box was calculated with the aim of reproducing the experimental density of the percentage of interest.

III. RESULTS AND DISCUSSION

The comparison between the computational and the experimental densities of the three systems (EAN+water, EAN+ethanol, and EAN+methanol) at room temperature is shown in Fig. 1 as a function of the solvent molar percentage, $\%_{solvent}$. The experimental density for the mixture of

24 February 2026 13:02:40

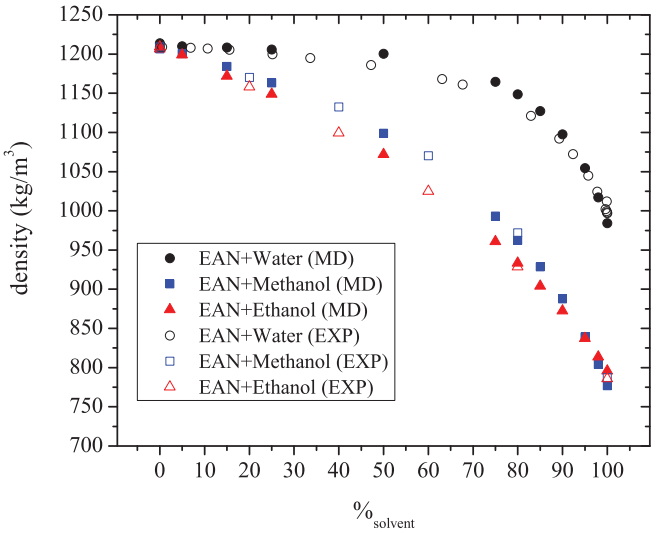

FIG. 1. Simulated (solid symbols) and experimental (open symbols) densities at $T = 298.15$ K of EAN mixed with water (circles), ethanol (triangles), and methanol (squares).

EAN with water was determined by Allen *et al.*,[47] whereas those corresponding to both mixtures with alcohols were measured in our laboratory, since no experimental data were found in the literature. As it can be seen, the agreement between our computational and experimental data is excellent over the whole composition range, which, according to current consensus,[62,63] is a good indicator that our parameterization captures the essential structural properties of the systems. Only a slight overestimation (ca. 2%) is registered at intermediate concentrations in the case of aqueous mixtures, which could be associated with the non-polarizable nature of the OPLS-AA potential. However, the use of non-polarizable force fields for equilibrium calculations is well established,[64,65] and is also the choice in this paper. EAN shows a similar response with the addition of both alcohols, whereas the transition from the density of pure EAN to pure water seems to be more gradual.

With the aim of studying the spatial correlations of the molecules in the bulk mixtures we have calculated the rdfs

$$g_{ii}(\vec{r}) = \frac{N}{\rho N_i^2}\left\langle \sum_{\alpha=1}^{N_i}\sum_{\beta\neq\alpha}^{N_i}\delta(\vec{r}+\vec{r}_\beta-\vec{r}_\alpha)\right\rangle,$$
$$g_{ij}(\vec{r}) = \frac{N}{\rho N_i N_j}\left\langle \sum_{\alpha=1}^{N_i}\sum_{\beta\neq\alpha}^{N_j}\delta(\vec{r}+\vec{r}_\beta-\vec{r}_\alpha)\right\rangle \quad i\neq j, \tag{1}$$

where N is the total number of particles, N_μ is the number of particles of species μ in the system, ρ stands for its number density, α and β run over all the particles, and brackets indicate the ensemble average. Unless explicitly stated otherwise, all the rdfs presented here have been calculated for the centers of mass of the corresponding ionic and molecular species. In Figs. 2, 3, and 5, we represent, respectively, the rdfs of water and alcohol with the different molecular species in the mixture, and cation-anion $g(r)$'s in the studied mixtures for the various reported concentrations. Probably, the most notable effect in Fig. 2 is the low degree of clustering of water molecules even at high cosolvent concentrations. Water hydrates the polar head of the cation, $[NH_3]^+$, in preference to $[NO_3]^-$. While the preferred water-$[NH_3]^+$ distance is 0.28 nm, $[NO_3]^-$ is relegated to a second layer further apart, at 0.35 nm. At low water concentrations, two layers of water around the central molecule are registered in Fig. 2(a).

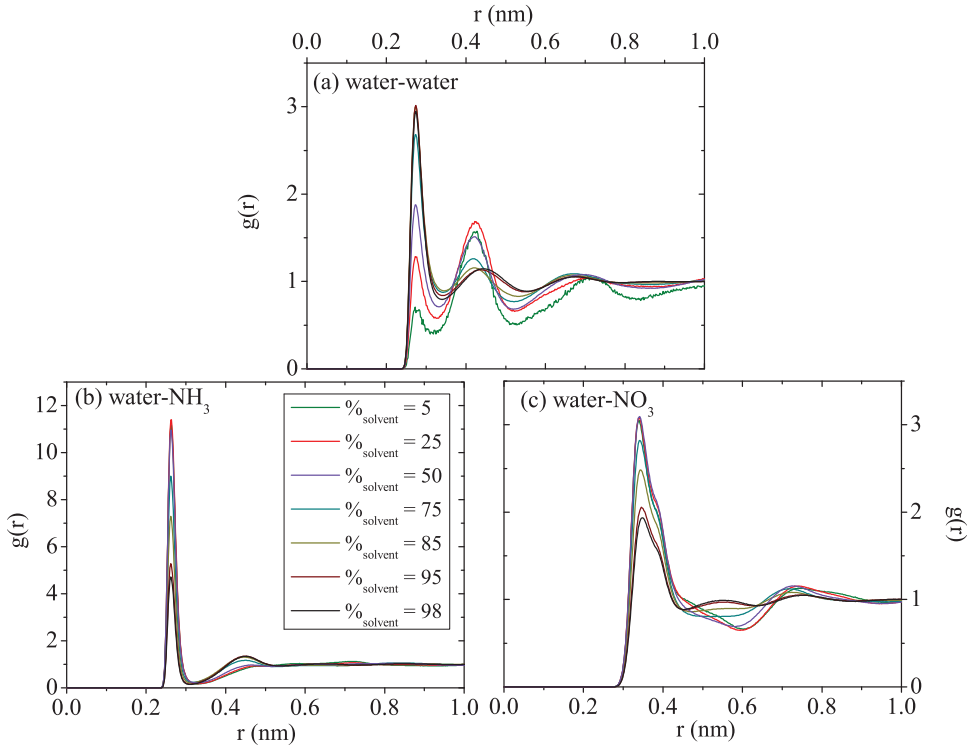

FIG. 2. Water concentration dependence of water-water (a), water-cation (b), and water-anion (c) rdfs in aqueous EAN mixtures at 298.15 K and 1 atm.

24 February 2026 13:02:40

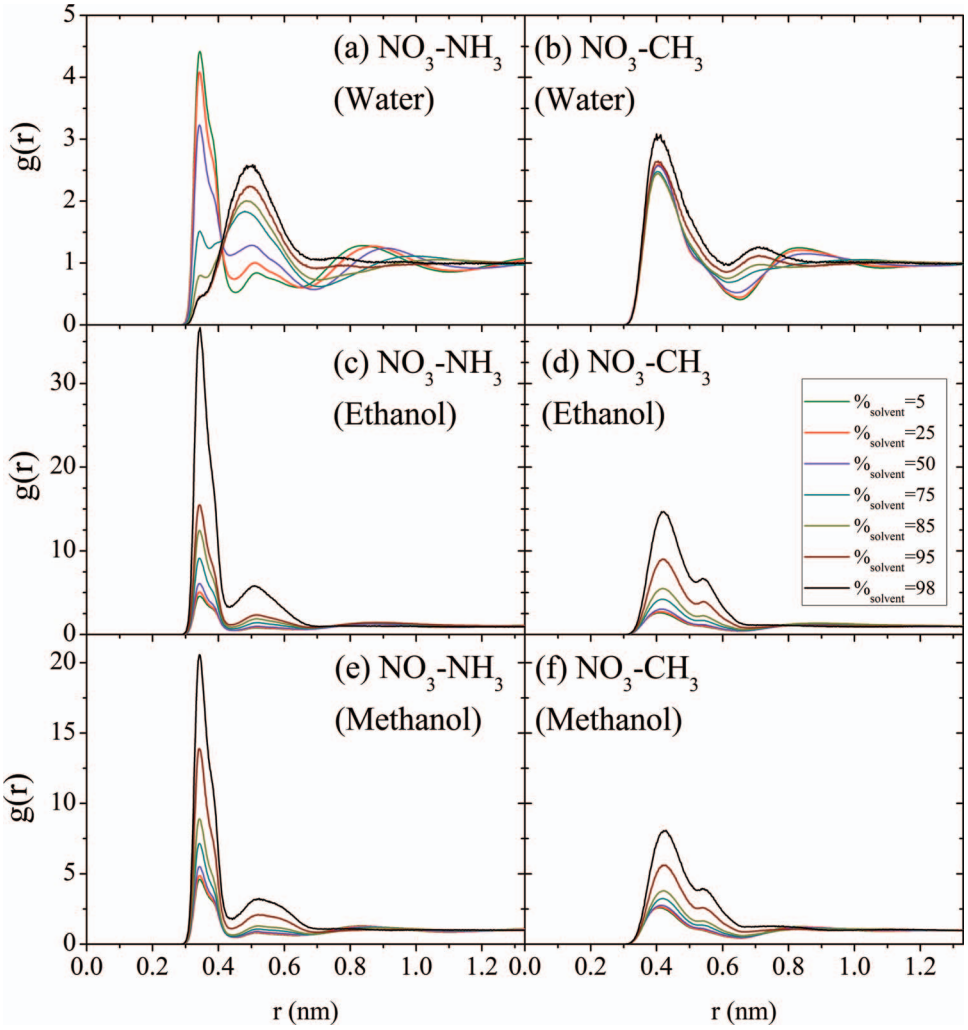

FIG. 3. (a)–(e) Cosolvent concentration dependence of anion-cation rdfs for EAN at 298.15 K and 1 atm.

The first one is placed at 0.38 nm of the central molecule and a second coordination layer is detected at 0.41 nm. The first peak is reinforced as concentration increases, while the second is progressively reduced by water addition. This water reorganization induces a structural transition in the mixture, with water replacing $[NO_3]^-$ in the first coordination layer of the polar head of the IL cation, something which can also be observed in the anion-cation rdf in water mixtures in Fig. 3(a). In this representation, this phenomenon seems to take place somewhere between 50% and 75% water concentration. In this concentration range, the first peak of the anion-cation $g(r)$ suffers a displacement from 0.30 nm to about 0.40 nm, indicating that $[NO_3]^-$ is expelled from the first solvation layer of the $[NH_3]^+$ groups. Another interesting feature is that during this structural transition $[NO_3]^-$ is displaced from the ammonium groups and approaches the alkyl side chain of the cations, as can be observed in Fig. 3, where a displacement of the second peak of the $[NO_3]^-$-$[CH_3]$ rdf from 0.9 nm to 0.75 nm can be seen. As for cation hydration, a trend of diminished intensity of the first peak can be observed with water addition, reflecting the increased affinity of the system for water-water coordination. Contrary to what has been reported for hydrophobic AILs[62,66] where water is highly clusterized at all concentrations, in our case the highest values of the first peak of the water-water rdf are quite low and, somewhat surprisingly, lower than the corresponding peaks of the water-cation rdfs, so we conclude that no water network is formed in aqueous mixtures of this PIL until quite large water concentrations, i.e., water seems to adopt a quite homogeneous distribution in the IL network.

This phenomenon can be further clarified if we analyze the evolution of the relative heights of the second and first peaks of the water-water and cation-anion rdfs. As can be seen in Fig. 4, the system progressively evolves from a small water clusters state (low water concentration) into a conventional aqueous solution where IL ions are hydrated in the usual way (high water concentration regime). If we adopt as a criterion for the transition the equalness of the height of the first and second rdf peaks, the transition gradually takes place between 40% and 70% water concentration, where the replacement of IL anions in the first solvation shell of the cations seems to be complete. Hence, we can assign the center of this concentration interval, a 55% water concentration, to the structural transition.

As regards the IL-alcohol mixtures in Fig. 5, monotonic increases of the first peaks of all the calculated rdfs are registered upon cosolvent addition in mixtures with ethanol. Contrarily to what some of us previously reported for AILs,[66]

24 February 2026 13:02:40

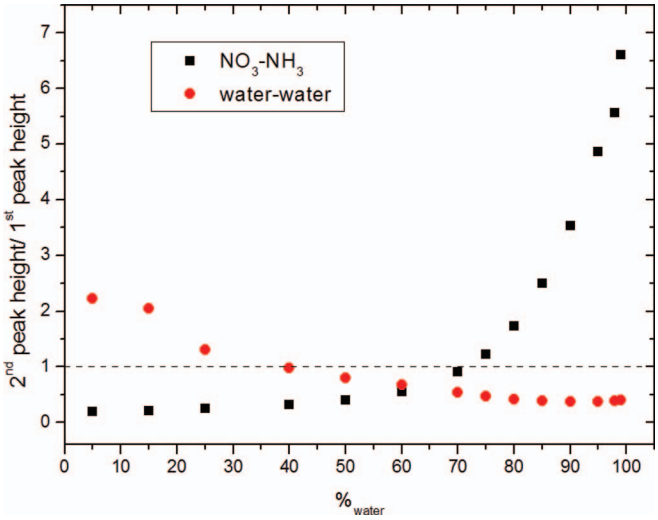

FIG. 4. Water concentration dependence of the relative heights of water-water (circles) and cation-anion (squares) in mixtures with EAN at 298.15 K and 1 atm.

no inversion is registered in the evolution of the height of the first peak of the anion-ethanol rdfs. The first peaks of all the ethanol-molecule rdfs increase monotonically with increasing alcohol concentration, indicating enhanced correlations of the cosolvent molecules with all the species in the bulk mixtures, in marked contrast to what happens in previously reported results for alcohol-AIL mixtures and in aqueous mixtures, where only the water-water rdf peak increases with cosolvent addition.[67] Besides, the second peak of the rdfs of ethanol with the IL anion is progressively weakened out by the addition of alcohol, reflecting a destructuring of the solvation shells of the anions beyond the first one. In the case of methanol-anion rdfs, this same behavior of the first and second peaks is also registered.

In the case of alcohol-cation rdfs, monotonic increases of the height of the first peak are also observed in Figs. 5(c) and 5(d), reflecting a clustering process of the alcohols around the polar heads of the cations. The second peaks also show similar behavior, although somehow more marked in the case of ethanol mixtures: a progressive weakening of the second shell is followed, at high cosolvent concentrations, by the formation of a second solvation shell of the cations by both ethanol and methanol, as indicated by the increase of the second peak height and its displacement towards lower distances. Finally, a monotonic increase of the first peak of the cosolvent-cosolvent rdf is registered in the case of mixtures with ethanol, but this is not the case for methanol. In the latter, an initial decrease of the height of the second peak is followed by an increase of the correlation as methanol concentration

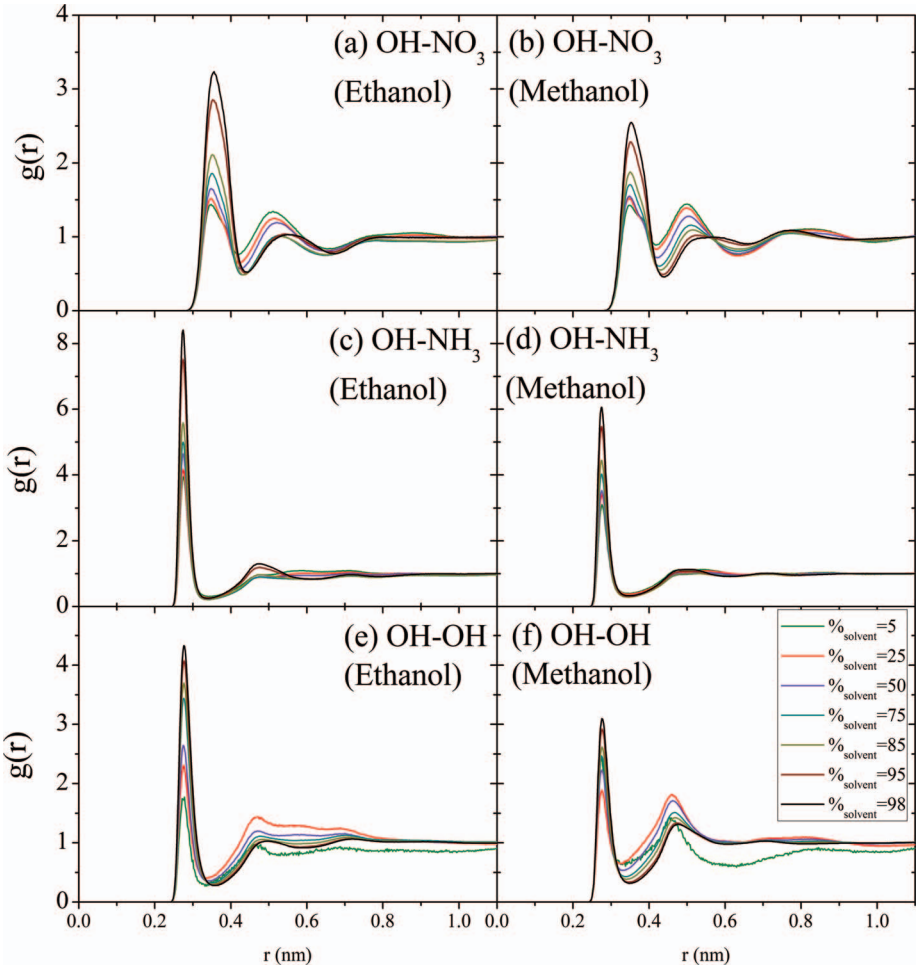

FIG. 5. Alcohol concentration dependence of alcohol-anion (a) and (b), alcohol-cation (c) and (d), and alcohol-alcohol (e) and (f) rdfs in ethanol and methanol mixtures with EAN at 298.15 K and 1 atm.

24 February 2026 13:02:40

increases, probably due to the lower ability of methanol to accommodate into the network of the IL. Notwithstanding, the second peak of both rdfs shows the same behavior for both alcohol species: an initial increase of the correlation from 5% to 25% is followed by a progressive weakening of the second coordination shell. As can be seen in Fig. 5, similar to the case of water mixtures, alcohol molecules also seem to have a marked preference for the cation polar head rather than by forming clusters or by solvating the anion all throughout the concentration range, although this tendency is not as marked as in the aqueous case. Despite the increasing trend of alcohol-alcohol correlations with increasing alcohol concentration, as shown by the height of the first peaks of $g_{\mathrm{OH-OH}}(r)$ for both alcohols, no evident alcohol cluster formation is observed since even at the highest concentrations of alcohol the first peak of the cation-alcohol rdf reaches double the height of that of the alcohol-alcohol $g(r)$. Besides, the correlations of alcohol molecules with IL cations and anions also increase with alcohol concentration, this tendency being more pronounced in the case of the alcohol with the longest side chain. Nevertheless, this evolution of alcohol structuring in the mixtures is not accompanied by a replacement of the IL anions in the first solvation layer of the IL cation (Figs. 3(c) and 3(e)), so structural transitions in the IL similar to those in EAN-water mixtures are not detected. This is indicative of ethanol molecules accommodating into the structure of the bulk PIL without significant perturbation of the latter. Finally, we will outline that the trends observed for the rdfs of both studied alcohols are qualitatively very similar. Only quantitative differences are registered, the most visible one being that of methanol at low alcohol concentrations, where the second peak at 0.48 nm is even higher than the first one at 0.29 nm (as in the water case). However, no marked structural transitions are detected in the cation-anion rfds upon alcohol addition, in marked contrast to the results for water mixtures.

To sum up, the overall picture emerging from the rdfs indicates that the addition of cosolvents to this PIL produces homogeneous distributions of water and alcohol molecules in the bulk, with no detection of significant clustering degrees even in the aqueous mixtures, oppositely to water-AILs mixtures.[66] The analysis of the rdfs indicates that both water and alcohols interact preferentially with the IL cation, in marked contrast with previous computational studies for AIL-cosolvent mixtures.[67,68] This must be related to the protic character of the IL allowing the insertion of cosolvent molecules in the hydrogen-bonded network of the IL species. This hydrogen bonding possibility in the PIL is presumably also responsible for the structural reorganization of the mixture with the addition of water taking place between 40% and 70% water concentration, upon which $[NO_3]^-$ is replaced by water in the first solvation layer of the cation polar head. On the other hand, the addition of ethanol or methanol preserves the overall structure of this PIL, only monotonic increases of the peaks being registered with no significant reorganization of the polar domains of the amphiphilically nanostructured PIL up to very high cosolvent concentrations. This difference between the cosolvents is associated with the different number of hydrogen bonds that water and alcohols can form.

This image of cosolvent homogeneously accommodating to the hydrogen bond network of the PILs upon mixing is reinforced by an analysis of the coordination numbers of the different species. These quantities are represented in Fig. 6. The most usual way for evaluating coordination numbers in the literature is by numerical integration of $4\pi r^2 g(r)$ up to its first minimum. In order to test our results, we computed the coordination numbers of cosolvent/IL mixtures over the whole range of cosolvent concentrations, obtained by integration of the first peak of the rdfs of the center of mass of the molecules, the least biased choice of distribution function. As one can see in the representation, IL anions are progressively solvated by water and alcohols until they reach limiting values of 6.1, 4.1, and 4.4 for water, ethanol, and methanol, respectively. The same behavior is registered for cations, for which the corresponding values are 3.3, 2.0, and 2.1. As expected, monotonic increases are registered in the coordination numbers of cosolvent-cosolvent molecules in all cases as cosolvent concentration increases, reaching in this case limiting values of 4.3, 2.5, and 2.6 for water, ethanol, and methanol, respectively. In the case of mixtures with alcohols, the coordination numbers calculated by integration of the first peak of the rdf are 2.6 and 2.1 for pure methanol and ethanol, respectively, in the case of O–O pairs, and 1.1 and 0.8 when

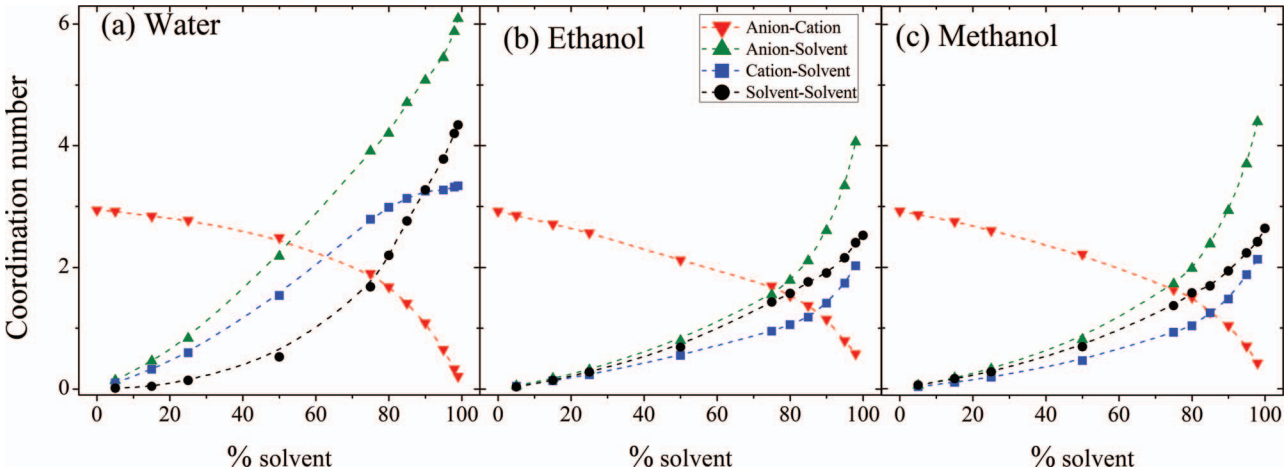

FIG. 6. Coordination numbers of water (a), ethanol (b), and methanol (c) in mixtures with EAN at 298.15 K. The lines are guides to the eye.

24 February 2026 13:02:40

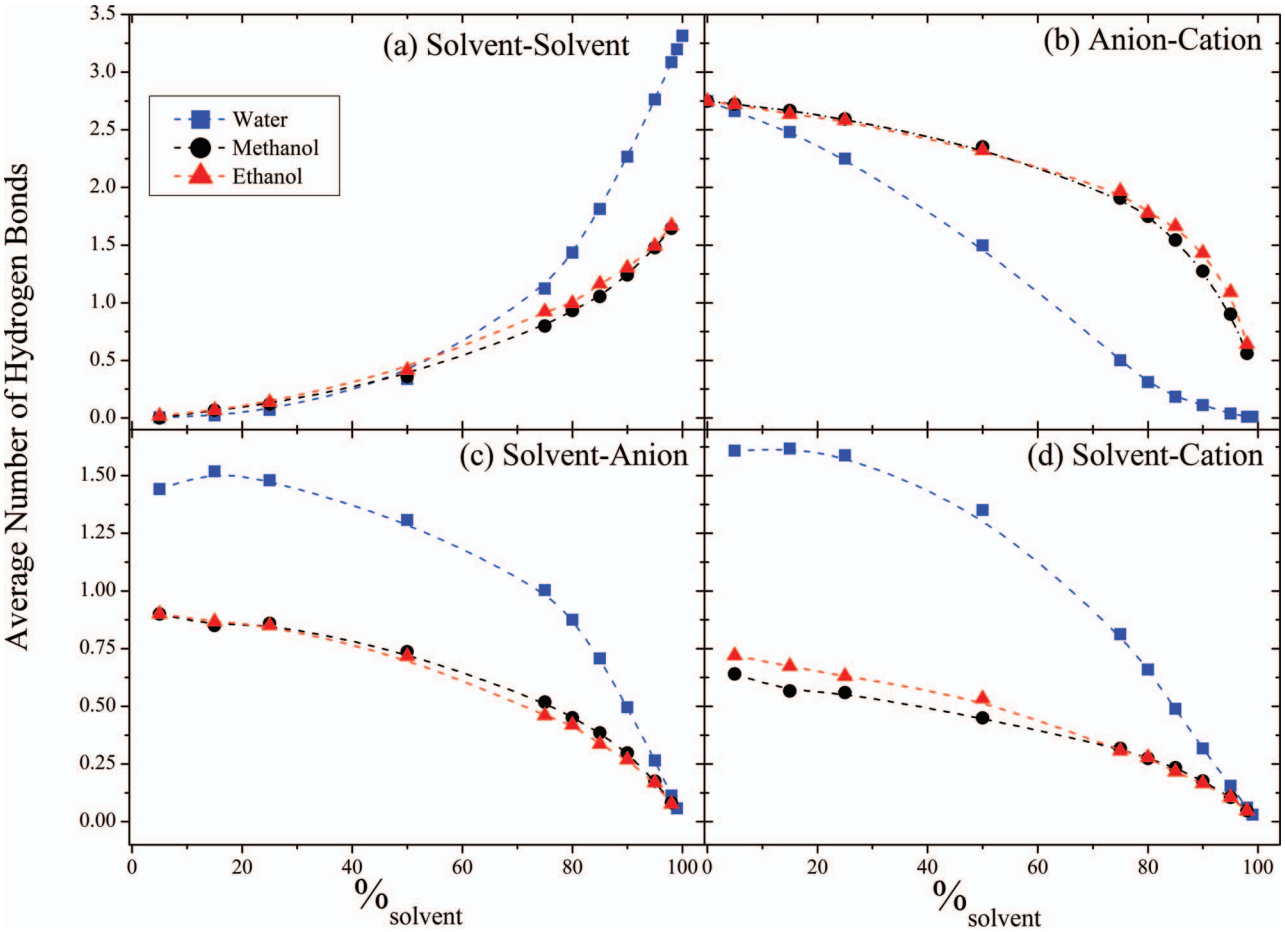

FIG. 7. Concentration dependence of the average number of cosolvent-cosolvent (a), cation-anion (b), cosolvent-cation (c), and cosolvent-anion (d) hydrogen bonds per molecule for mixtures with EAN at 298.15 K. The lines are guides to the eye.

using O–H pairs,[67] the latter in good agreement to those of Saiz *et al.* (2 and 1 for O–O and O–H pairs).[43]

As regards hydrogen bonds between the various species in the mixture, they are represented for the different species in the studied mixtures in Fig. 7. As it is well known, computationally we can use a geometrical or an energetic criterion for defining a "hydrogen bond."[44] According to Ref. 44, a pair of molecules are considered H-bonded if the distance between the hydrogen and the acceptor is smaller than 0.35 nm and the angle of the donor-hydrogen-acceptor is less than 30°. In this work, we use the criterion implemented in GROMACS, where OH and NH groups are regarded as donors, and O and N are considered to be acceptors. We can see in Fig. 7 that the number of hydrogen bonds between cosolvent molecules monotonically increases with dilution of the PIL, as expected, reaching the values of 3.3, 1.7, and 1.6 for pure water, ethanol and methanol, respectively, in agreement with those previously reported.[66,67] For mixtures with water, some of us reported values of ca. 3.5 hydrogen bonds per water molecule in Ref. 66, close to the four hydrogen bonds of most water molecules in the liquid phase.[41,42,69] On the other hand, the average number of alcohol-alcohol hydrogen bonds in the pure systems was computed to be 1.82 for both ethanol and methanol.[67] Cation-anion hydrogen bonds decrease much more rapidly in water-IL mixtures than in the corresponding alcohol ones, and in aqueous environment they exhibit an inflection point ca. 50% water concentration – hence near the concentration for the structural transition previously mentioned in the analysis of the rdfs – while in alcohol mixtures the function is concave all throughout the concentration range. This confirms that water induces a replacement of anions in the first solvation shell of the cation, but alcohols are not capable of doing so, as we observed in the rdfs analysis above. Moreover, Figs. 7(c) and 7(d) show that the number of hydrogen bonds of cosolvent molecules with IL anions and cations have very different behavior in aqueous or alcoholic mixtures: while in the former case maxima of the number of hydrogen bonds are registered for both ionic species, monotonic decreases are predicted for cation- and anion-cosolvent hydrogen bond numbers per molecule. This confirms once again the structural transition in aqueous mixtures associated with a restructuring of the first solvation layer of the cation polar head.

In order to obtain a three-dimensional picture of the structural distribution of the molecules in the bulk, we calculated the angular dependence of the probability distribution of finding a molecule at a given distance from another one, the so-called spatial distribution functions (sdfs). These highlight the regions where finding a given species around a central molecule at a fixed distance is more probable. The result is depicted in Fig. 8 in the form of heat maps for the various cosolvent molecules analyzed in this paper at concentrations

24 February 2026 13:02:40

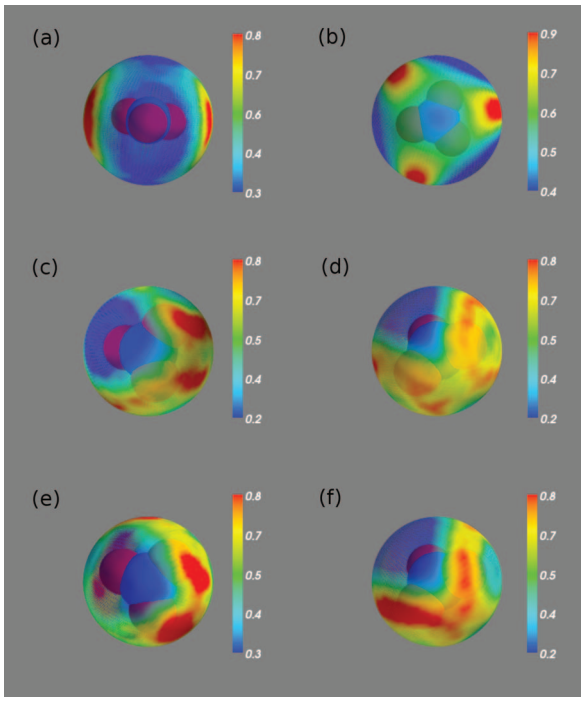

FIG. 8. Spatial distribution functions of water (a) and (b), ethanol (c) and (d), and methanol (e) and (f) around anions in mixtures with EAN at 298.15 K. The pictures on the left column correspond to a concentration of 25% and those on the right to 85%.

of 25% and 85%, chosen to be well below and above the structural transition detected in water mixtures. The chosen distances always correspond to the first peak of the corresponding rdfs. The behaviors of water and alcohol molecules are clearly different. The former tends to coordinate to $[NO_3]^-$ in a bidentate fashion in the bisectrices of the anion molecules at low concentrations and progressively occupy the polar regions of the sphere. However, alcohol molecules coordinate oxygen atoms in a monodentate way at low concentrations, and tend to compete for them at high concentrations, giving rise to the formation of spherical rings around these atoms.

The effect of the surroundings on the properties of the molecules and the possible formation of stable and long-lived aggregates that involve cosolvent molecules and IL anions on its first solvation shell can also be described by a calculation of the velocity autocorrelation function (vacf),

$$C(t) = \frac{\langle \vec{v}(t) \cdot \vec{v}(0) \rangle}{\langle \vec{v}(0) \cdot \vec{v}(0) \rangle}, \tag{2}$$

where $\vec{v}(t)$ is the velocity of the center of mass of the molecule at time t and the angle brackets indicate an ensemble average. We analyzed the single-particle dynamics of these solutions by means of the study of the center-of-mass vacfs of water and alcohol molecules, and the result is represented in Fig. 9, where we plot the concentration dependence of the vacfs of

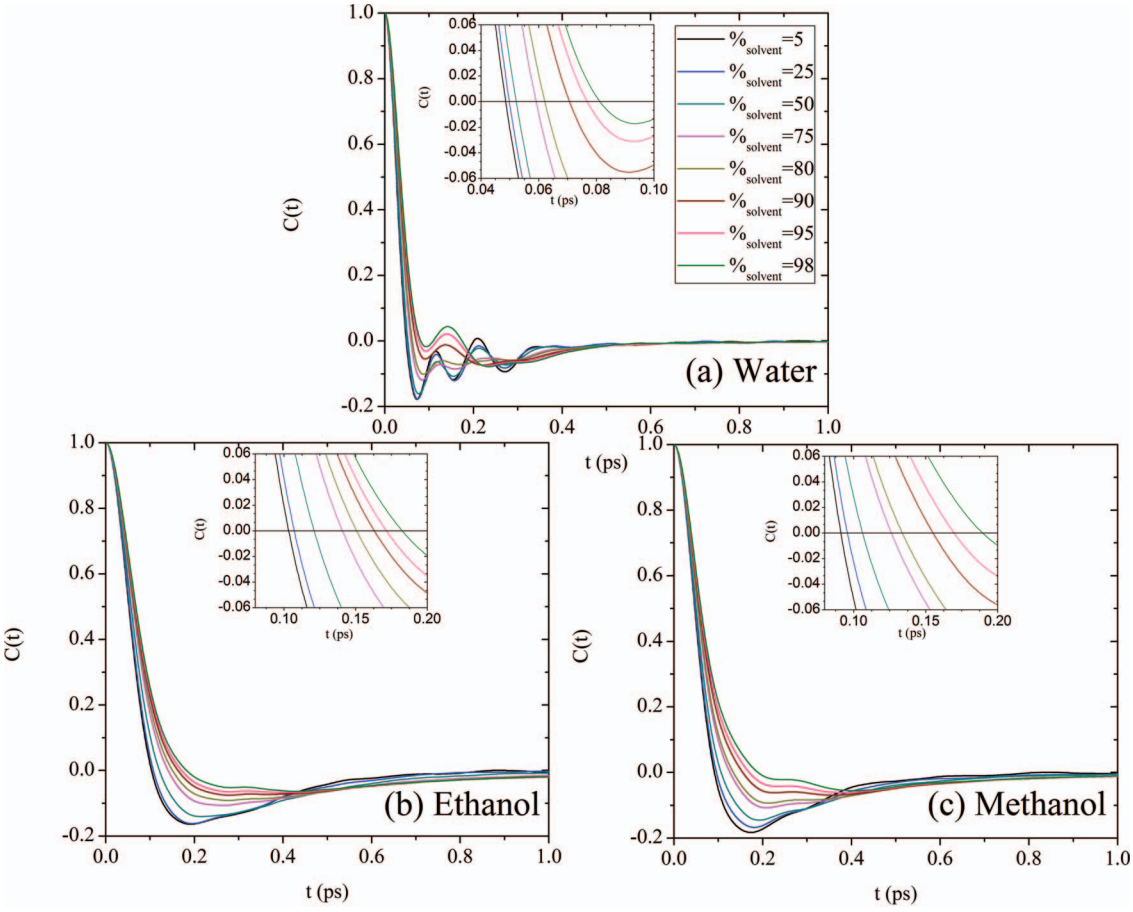

FIG. 9. Concentration dependence of water (a), ethanol (b), and methanol (c) vacfs in solutions with EAN. The insets show the evolution of the collision time with the concentration of cosolvent molecules. The statistical uncertainties of $C(t)$ in the time intervals of the insets are expected to be less than 10^{-4}.

24 February 2026 13:02:40

these cosolvent molecules in the solutions with EAN. As can be seen in that representation, water molecules undergo a "rattling" motion in cages formed by their nearest neighbor molecules in the bulk solutions, as revealed by the oscillations of their vacfs. This type of motion is also observed for AILs[66] and is indicative of water molecules being quite tightly bound to their neighbours, with which they collide and rebound, inverting their velocities. Besides, we can observe that these correlations are almost completely damped out within ca. 0.4 ps. As water concentration increases, water vacf is progressively smoothed out until values for pure water are recovered, as previously reported,[66,70,71] and the amplitude of the oscillations decreases with water addition in opposition to what happens to the collision time.

The same behavior is not registered for alcohol molecules, for which oscillations fade away shortly after the first highly damped minimum of their vacf. This is characteristic of a diffusive motion of ethanol and methanol molecules rapidly setting in and destroying any oscillatory behavior of the vacfs associated with correlations between the molecules. This is also the type of single-particle dynamics registered for mixtures of AILs and alcohols,[72] and here we also found collision times increasing with alcohol concentrations. The vacfs also decay in a subpicosecond scale, and the mean collision time given by the first zero of the vacf increases with the addition of alcohol to the mixture for both alcohols until their pure values (ca. 0.21 ps for ethanol and 0.28 ps for methanol) are reached. Besides, as in the case of aqueous solutions, the value of the vacf at the first minimum increases and is registered at longer times, indicating a progressive weakening of the correlations of the cosolvent molecules with their surrounding IL ions and cosolvent molecules. In these mixtures, the velocity correlations are completely destroyed beyond 0.5 ps, a slightly lower threshold than in similar AIL-alcohol mixtures.[72] All this suggests that water molecules are more tightly bound in the hydrogen-bonded network than alcohol ones, as one would expect due to their different number of possible hydrogen bonds.

IV. CONCLUSIONS

We computationally analyzed the structure of mixtures of a PIL, EAN, with water and two alcohols, ethanol and methanol, by calculating several equilibrium quantities (density, rdfs, coordination numbers, and hydrogen bonds) and their single-particle dynamics (vacfs). The overall resulting picture indicates that, contrary to what happens in AILs, the added polar molecules tend to accommodate into the pre-existing hydrogen-bonded network of the PIL, giving rise to homogeneous distributions throughout all the concentration range. The formation of cosolvent networks is not observed in the studied mixtures with PILS (in contrast to mixtures with AILs), and even in aqueous mixtures water seems to prefer hydrating the cation polar head. However, water still forms hydrogen bonds with both species, as suggested by the number of hydrogen bonds to anions being greater than that to cations. Moreover, we detected a structural transition at about 55% in aqueous mixtures, associated with $[NO_3]^-$ being expelled by water molecules from the first solvation layer of the polar heads of the cations, which is not observed in the mixtures with alcohols. In addition, the spatial distribution functions also reveal differences between aqueous and alcohol mixtures: while in the former water coordinates anions in a bidentate fashion in the bisectrices of the molecular equatorial plane at all concentrations, alcohols show a strong preference for coordinating with the oxygen atoms in a monodentate way, competing for these atoms at high concentrations and leading to the appearance of spherical rings in the sdfs around them. Finally, as far as single-particle dynamics is concerned, water molecules are seen to be more strongly caged by the neighbours than alcohol molecules, a consequence of the tighter hydrogen bonding of water.

To sum up, the possibility of hydrogen bond formation of both water and alcohols in PIL mixtures induces the formation of a mixed network of IL and cosolvent molecules that progressively replace each other as the concentration of the mixture changes. This is in marked contrast to the formation of segregated networks in mixtures with AILs.

ACKNOWLEDGMENTS

The authors wish to thank the financial support of Xunta de Galicia through the research projects of references 10-PXIB-103-294 PR, 10-PXIB-206-294 PR and GPC2013-043. Moreover, this work was funded by the Spanish Ministry of Science and Innovation (Grant No. FIS2012-33126). All these research projects are partially supported by FEDER. T. Méndez-Morales thanks the Spanish ministry of Education for her FPU grant. Facilities provided by the Galician Supercomputing Centre (CESGA) are also acknowledged.

[1] M. Armand, F. Endres, D. R. MacFarlane, H. Ohno, and B. Scrosati, Nat. Mater. **8**, 621 (2009).
[2] N. V. Plechkova and K. R. Seddon, Chem. Soc. Rev. **37**, 123 (2008).
[3] H. Zhao and S. V. Malhotra, Aldrichim. Acta **35**, 75 (2002).
[4] R. D. Rogers and K. R. Seddon, *Ionic Liquids: Industrial Applications for Green Chemistry* (American Chemical Society, 2002).
[5] S. Zhang, N. Sun, X. He, X. Lu, and X. Zhang, J. Phys. Chem. Ref. Data **35**, 1475 (2006).
[6] M. Freemantle, *An Introduction to Ionic Liquids* (RSC Publishing, 2009).
[7] P. Wasserscheid and T. Welton, *Ionic Liquids in Synthesis* (Wiley Online Library, 2003).
[8] S. Zhang, X. Lu, Q. Zhou, X. Li, X. Zhang, and S. Li, *Ionic Liquids: Physicochemical Properties* (Elsevier, 2009).
[9] T. L. Greaves and C. J. Drummond, Chem. Rev. **108**, 206 (2008).
[10] W. X. M. Yoshizawa and C. A. Angell, J. Am. Chem. Soc. **125**, 15411 (2003).
[11] C. A. Angell, N. Byrne, and J.-P. Belieres, Acc. Chem. Res. **40**, 1228 (2007).
[12] T. L. Greaves, A. Weerawardena, C. Fong, I. Krodkiewska, and C. J. Drummond, J. Phys. Chem. B **110**, 22479 (2006).
[13] H. Nakamoto and M. Watanabe, Chem. Commun. **2007**, 2539.
[14] M. A. B. H. Susan, A. Noda, S. Mitsushima, and M. Watanabe, Chem. Commun. **2003**, 938.
[15] L. Timperman, P. Skowron, A. Boisset, H. Galiano, D. Lemordant, E. Frackowiak, F. Beguinb, and M. Anouti, Phys. Chem. Chem. Phys. **14**, 8199 (2012).
[16] M. Anouti and L. Timperman, Phys. Chem. Chem. Phys. **15**, 6539 (2013).
[17] S. Menne, J. Pires, M. Anouti, and A. Balducci, Electrochem. Commun. **31**, 39 (2013).
[18] P. Walden, Bull. Russian Acad. Sci. **1800**, 405 (1914).
[19] V. H. Alvarez, N. Dosil, R. Gonzalez-Cabaleiro, S. Mattedi, M. Martin-Pastor, M. Iglesias, and J. M. Navaza, J. Chem. Eng. Data **55**, 625 (2010).

24 February 2026 13:02:40

[20]B. Fernández-Castro, T. Méndez-Morales, J. Carrete, E. Fazer, O. Cabeza, J. R. Rodríguez, M. Turmine, and L. M. Varela, J. Phys. Chem. B **115**, 8145 (2011).
[21]S. Bouzón-Capelo, T. Méndez-Morales, J. Carrete, E. L. Lago, J. Vila, O. Cabeza, J. R. Rodríguez, M. Turmine, and L. M. Varela, J. Phys. Chem. B **116**, 11302 (2012).
[22]R. Atkin and G. G. Warr, J. Phys. Chem. B **112**, 4164 (2008).
[23]R. Atkin, S. M. C. Bobillier, and G. G. Warr, J. Phys. Chem. B **114**, 1350 (2010).
[24]R. Hayes, S. Imberti, G. G. Warr, and R. Atkin, Phys. Chem. Chem. Phys. **13**, 13544 (2011).
[25]J. Hunger, T. Sonnleitner, L. Liu, R. Buchner, M. Bonn, and H. J. Bakker, J. Phys. Chem. Lett. **3**, 3034 (2012).
[26]R. Hayes, S. Imberti, G. G. Warr, and R. Atkin, Phys. Chem. Chem. Phys. **13**, 3237 (2011).
[27]D. F. Kennedy and C. J. Drummond, J. Phys. Chem. B **113**, 5690 (2009).
[28]P. Niga, D. Wakeham, A. Nelson, G. G. Warr, M. Rutland, and R. Atkin, Langmuir **26**, 8282 (2010).
[29]X. C. X. Wang, Q. Li, and Z. Li, Langmuir **28**, 16547 (2012).
[30]C. Zhao, G. Burrell, A. A. J. Torriero, F. Separovic, N. F. Dunlop, D. R. MacFarlane, and A. M. Bond, J. Phys. Chem. B **112**, 6923 (2008).
[31]T. L. Greaves, A. Weerawardena, I. Krodkiewska, and C. J. Drummond, J. Phys. Chem. B **112**, 896 (2008).
[32]T. L. Greaves, A. Weerawardena, C. Fong, and C. J. Drummond, J. Phys. Chem. B **111**, 4082 (2007).
[33]E. Bodo, P. Postorino, S. Mangialardo, G. Piacente, F. Ramondo, F. Bosi, P. Ballirano, and R. Caminiti, J. Phys. Chem. B **115**, 13149 (2011).
[34]H. Markusson, J.-P. Belieres, P. Johansson, C. A. Angell, and P. Jacobsson, J. Phys. Chem. A **111**, 8717 (2007).
[35]E. Bodo, S. Mangialardo, F. Ramondo, F. Ceccacci, and P. Postorino, J. Phys. Chem. B **116**, 13878 (2012).
[36]X. Song, H. Hamano, B. Minofar, R. Kanzaki, K. Fujii, Y. Kameda, S. Kohara, M. Watanabe, S. Ishiguro, and Y. Umebayashi, J. Phys. Chem. B **116**, 2801 (2012).
[37]Y. Umebayashi, W.-L. Chung, T. Mitsugi, S. Fukuda, M. Takeuchi, K. Fujii, T. Takamuku, R. Kanzaki, and S. Ishiguro, J. Comput. Chem. Jpn. **7**, 125 (2008).
[38]S. Zahn, J. Thar, and B. Kirchner, J. Chem. Phys. **132**, 124506 (2010).
[39]K. Marsh, J. Boxall, and R. Lichtenthaler, Fluid Phase Equilib. **219**, 93 (2004).
[40]A. W. K. Fumino and R. Ludwig, Angew. Chem. Int. Ed. **48**, 3184 (2009).
[41]A. Luzar and D. Chandler, Phys. Rev. Lett. **76**, 928 (1996).
[42]F. H. Stillinger, Science **209**, 451 (1980).
[43]L. Saiz, J. A. Padro, and E. Guardia, J. Phys. Chem. B **101**, 78 (1997).
[44]M. Haughney, M. Ferrario, and I. R. McDonald, J. Phys. Chem. **91**, 4934 (1987).
[45]T. Yamaguchi, H. Hidaka, and A. K. Soper, Mol. Phys. **96**, 1159 (1999).
[46]M. Matsumoto and K. E. Gubbins, J. Chem. Phys. **93**, 1981 (1990).
[47]M. Allen, D. F. Evans, and R. Lumry, J. Sol. Chem. **14**, 549 (1985).
[48]T. J. V. Findlay and M. C. R. Symons, J. Chem. Soc., Faraday Trans. 2 **72**, 820 (1976).
[49]R. G. Horn, D. F. Evans, and B. W. Ninham, J. Phys. Chem. **92**, 3531 (1988).
[50]I. B. Malham, P. Letellier, A. Mayaffre, and M. Turmine, J. Chem. Thermodyn. **39**, 1132 (2007).
[51]S. Bouguerra, I. B. Malham, P. Letelliera, and M. T. A. Mayaffre, J. Chem. Thermodyn. **40**, 146 (2008).
[52]T. Heimburg, S. Z. Mirzaev, and U. Kaatze, Phys. Rev. E **62**, 4963 (2000).
[53]A. Chagnes, A. Tougui, B. Carre, N. Ranganathan, and D. Lemordant, J. Sol. Chem. **33**, 247 (2004).
[54]T. L. Greaves, D. F. Kennedy, A. Weerawardena, N. M. K. Tse, N. Kirby, and C. J. Drummond, J. Phys. Chem. B **115**, 2055 (2011).
[55]T. L. Greaves, D. F. Kennedy, N. Kirbyb, and C. J. Drummond, Phys. Chem. Chem. Phys. **13**, 13501 (2011).
[56]R. Hayes, S. Imberti, G. G. Warr, and R. Atkin, Angew. Chem. Int. Ed. **51**, 7468 (2012).
[57]D. V. D. Spoel, E. Lindahl, B. Hess, A. R. V. Buuren, E. Apol, P. J. Meulenhoff, D. P. Tieleman, A. L. T. M. Sijbers, K. A. Feenstra, R. V. Drunen, and H. J. C. Berendsen, *Gromacs User Manual Version 4.0*, see http://www.Gromacs.org, 2005.
[58]S. V. Sambasivarao and O. Acevedo, J. Chem. Theory Comput. **5**, 1038 (2009).
[59]M. W. Mahoney and W. L. Jorgensen, J. Chem. Phys. **112**, 8910 (2000).
[60]W. L. Jorgensen, D. S. Maxwell, and J. Tirado-Rives, J. Am. Chem. Soc. **118**, 11225 (1996).
[61]T. Méndez-Morales, J. Carrete, S. Bouzón-Capelo, M. Pérez-Rodríguez, O. Cabeza, L. J. Gallego, and L. M. Varela, J. Phys. Chem. B **117**, 3207 (2013).
[62]S. Feng and G. A. Voth, Fluid Phase Equilib. **294**, 148 (2010).
[63]G. Raabe and J. Köhler, J. Chem. Phys. **129**, 144503 (2008).
[64]J. N. Canongia-Lopes and A. A. H. Pádua, J. Phys. Chem. B **110**, 3330 (2006).
[65]W. Jiang, Y. Wang, and G. A. Voth, J. Phys. Chem. B **111**, 4812 (2007).
[66]T. Méndez-Morales, J. Carrete, O. Cabeza, L. J. Gallego, and L. M. Varela, J. Phys. Chem. B **115**, 6995 (2011).
[67]T. Méndez-Morales, J. Carrete, O. Cabeza, L. J. Gallego, and L. M. Varela, J. Phys. Chem. B **115**, 11170 (2011).
[68]J. N. Canongia-Lopes, M. F. Costa-Gomes, and A. A. H. Pádua, J. Phys. Chem. B **110**, 16816 (2006).
[69]J. H. Guo, Y. Luo, A. Augustsson, J. Rubensson, C. Sthe, H. gren, H. Siegbahn, and J. Nordgren, Phys. Rev. Lett. **89**, 137402 (2002).
[70]I. Harsnyi, L. Pusztai, J. C. Soetens, and P. A. Bopp, J. Mol. Liq. **129**, 80 (2006).
[71]M. Sokol, A. Dawid, Z. Dendzik, and Z. Gburski, J. Mol. Struct. **704**, 341 (2004).
[72]T. Méndez-Morales, J. Carrete, M. García, O. Cabeza, L. J. Gallego, and L. M. Varela, J. Phys. Chem. B **115**, 15313 (2011).

24 February 2026 13:02:40